A&A 411, L197–L201 (2003)
DOI: 10.1051/0004-6361:20031210

Astronomy & Astrophysics

In-flight performance of the IBIS calibration unit⋆

A. J. Bird[1], A. Bazzano[2], C. Ferguson[1], G. La Rosa[3], G. Malaguti[4], and P. Ubertini[2]

[1] School of Physics and Astronomy, University of Southampton, Highfield, Southampton, SO17 1BJ, UK
[2] Istituto di Astrofisica Spaziale e Fisica Cosmica, IASF/CNR, Rome, Italy
[3] Istituto di Astrofisica Spaziale e Fisica Cosmica, IASF/CNR, Sezione di Palermo, Palermo, Italy
[4] Istituto di Astrofisica Spaziale e Fisica Cosmica, IASF/CNR, Sezione di Bologna, Bologna, Italy

Received 11 July 2003 / Accepted 4 August 2003

Abstract. We describe the in-flight performance of the on-board calibration unit for the IBIS telescope on INTEGRAL. Both intrinsic performance and the quality of the calibration signals provided to the IBIS detector planes are discussed. The calibration unit intrinsic performance is assessed based on the diagnostic information in IBIS housekeeping. The flux of tagged photons, i.e. those arriving at the detector planes in coincidence with a calibration strobe, is assessed from in-flight data, and analysed in conjunction with a detailed simulation. Proposed usage of the tagged photon flux is discussed, and the expected calibration accuracy derived. The effect on science data from untagged calibration unit photons is assessed based on the predicted rate and distribution of such photons.

Key words. INTEGRAL – gamma-ray – calibration

1. Introduction

The IBIS telescope (Ubertini et al. 1996, 2003) on INTEGRAL (Winkler et al. 2003) includes a small in-flight calibration system designed to allow monitoring of the gains and overall performance of the individual detector components making up the ISGRI (Lebrun et al. 2003) and PICsIT (Labanti et al. 2003) detector planes and the active veto system (Quadrini et al. 2003). Here we describe the in-flight performance of the IBIS on-board calibration unit derived during telescope commissioning operations.

2. Principle of operation

The IBIS on-board calibration unit (OBCU) provides a continuous but small flux of 511 and 1275 keV photons to the detector planes, together with a logic signal (hereafter the "calibration strobe") which is interpreted by the detector planes as a signal that a calibration photon has been emitted. The calibration photons are thus recognised by the detector planes as coming from the OBCU due to their coincidence with the calibration strobe, and are diverted to dedicated calibration data streams, preventing contamination of the science data.

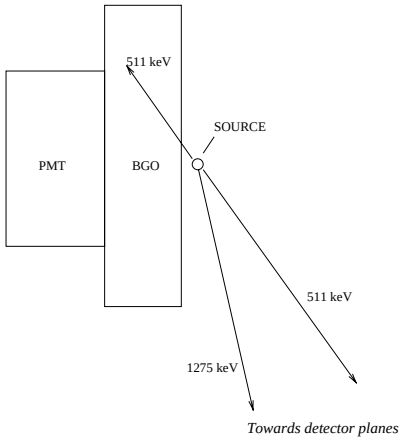

Fig. 1. Principle of IBIS OBCU operation: photons emitted towards the IBIS detector planes are "tagged" by simultaneous detections in the BGO tagging system.

The process of associating a calibration strobe with each emitted calibration photon is described as "tagging" the photon. The OBCU consists of an active tagging system based on a modified IBIS veto detector and a low intensity (0.4 μCi at launch) ^{22}Na radioactive source (Poulsen 2001). The ^{22}Na source disintegrations result in either two 511 keV and one 1275 keV photons (90% of the time) or just a 1275 keV photon (10% of the time). Since the two 511 keV photons are emitted 180° apart, the detection of one photon can be used to indicate a source disintegration while maintaining the photon flux towards the detector planes (see Fig. 1).

Send offprint requests to: A. J. Bird,
e-mail: ajb@astro.soton.ac.uk

⋆ Based on observations with INTEGRAL, an ESA project with instruments and science data centre funded by ESA member states (especially the PI countries: Denmark, France, Germany, Italy, Switzerland, Spain), Czech Republic and Poland, and with the participation of Russia and the USA.

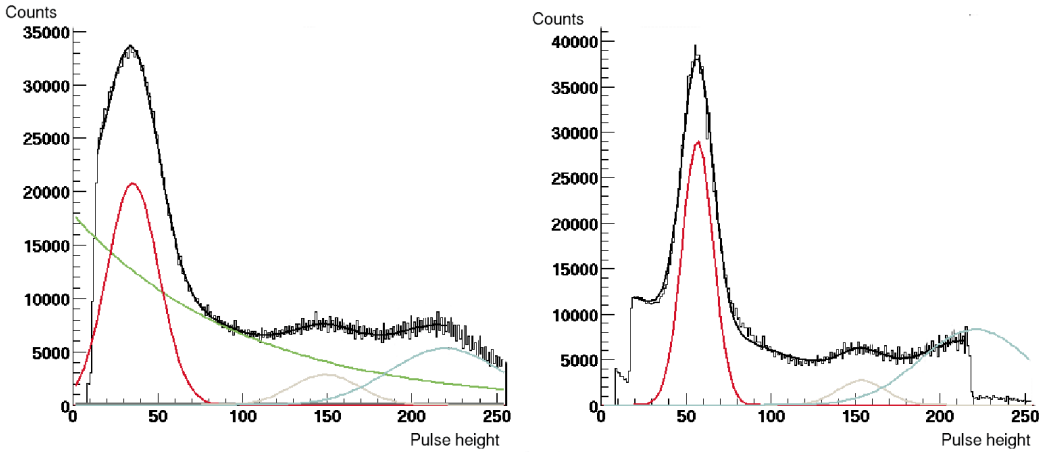

Fig. 2. Internal diagnostic pulse height spectra from the OBCU for (left) in-flight operation and (right) during ground calibrations. The individual Gaussian fits to the 511, 1275 and 1786 lines, together with an exponential background component, are shown together with the recorded spectrum.

The tagging system itself is based on a modified veto detector unit, which uses a 2 cm thick bismuth germanate (BGO) scintillator block as the active detection volume, viewed by two photomultipliers. The standard veto system electronics are modified, and an additional high voltage unit included, to provide the necessary redundancy against the failure of one photomultipler or high voltage supply. This detector system generates a calibration strobe, which is distributed to the detector planes, whenever the ^{22}Na calibration source generates an energy deposit between 100–2000 keV in the tagging system. Any events in the detector planes which are in coincidence with the 2 μs calibration strobe are recorded as calibration events.

3. Activation and commissioning

First activation commenced after 17 days in orbit, in order to allow for outgassing around the critical high voltage (HV) components. OBCU health was monitored via instrument housekeeping data. The BGO/PMT temperature was typically around −12 °C and the HV supply typically −1100 V.

The count rate in the OBCU tagging detector system, as reported in the instrument housekeeping data was 6120 c/s. This compares to a typical value of 9940 c/s observed during ground calibrations, and so indicated a significant deviation from the expected performance.

Instrument housekeeping also provides for the periodic transmission of a pulse height spectrum from the OBCU tagging system, which allows gain monitoring of the active components of the OBCU. Figure 2(left) shows a typical in-flight spectrum from the OBCU tagging detector. The three peaks visible in the spectrum correspond to the expected 511 keV, 1275 keV and 1786 (511+1275) keV peaks from the ^{22}Na source. However, comparing this to a typical spectrum recorded during ground calibration (Fig. 2, right), the in-flight spectrum shows significant departures from the on-ground behaviour,which may be considered as nominal. Note that the on-ground spectrum is taken in coincidence with the calibration strobe itself. This superimposes the thresholds for calibration strobe generation on the spectrum and causes the sharp discontinuities at pulse height channels ∼20 and ∼220.

The most significant difference is the broadening and shift of the 511 keV peak to a lower channel. In the ground spectrum, the lower side of the 511 keV peak is well above the tagging threshold, while in the flight spectrum, the threshold cuts into the peak. Conversely the two high-energy peaks are still in approximately the same channels.

Inspection of the channel-energy relations derived by fitting to the three peaks show that the relationship remains linear, but the peak shift is actually indicative of a large offset being present in the flight configuration. The total number of counts in the flight spectrum indicates a significantly lower BGO count rate compared to the ground data, which is consistent with the reduction seen in the housekeeping counters.

3.1. The blinding effect

The interpretation of this in-flight behaviour is that the tagging performance is significantly worse than that seen during ground calibrations. The most likely explanation is that the BGO tagging system is being degraded by the presence of a large high-energy particle flux, as seen in the other detectors (Segreto 2003). The modifications made to the veto electronics to avoid “blinding” was not made on the OBCU due to incompatibility with the need to support cold redundancy in the OBCU.

The high energy flux is creating two linked effects, which are illustrated in Fig. 3, and are sufficient to explain the deviations from nominal behaviour seen in the calibration unit performance reported in the housekeeping data.

1. The reduced count rate in the OBCU tagging detector indicates a large dead-time in that detector (since the ^{22}Na source intensity and position are fixed). During the readout of each energy deposit, the BGO tagging system or electronics will become saturated and unable to detect additional photons for a given time period. The dead time due to the photons from the calibration source itself is only of the order of 1%. However, the duration of the saturation will be

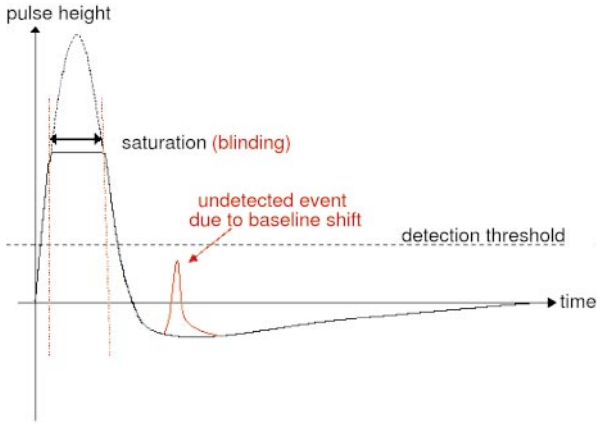

Fig. 3. Proposed saturation, blinding and baseline restoration effects in OBCU electronics due to the detection of high energy photons or charged particles.

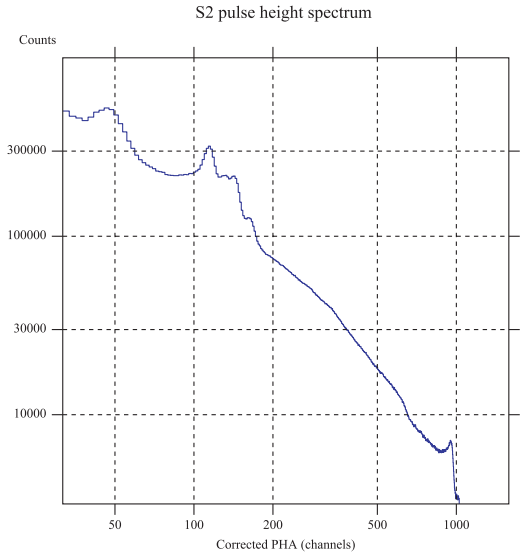

Fig. 4. Typical S2 (ISGRI calibration) spectrum summed over all pixels. PHA values have been gain-normalised, but charge loss correction has not been applied.

proportional to the detected energy, and so the detection of many high energy photons or charged particles will create a significant dead-time.

2. The shift in the peaks in the OBCU diagnostic spectra indicates a baseline restoration problem, almost certainly as a response to the detection of high energy events in the BGO scintillator. This could occur either in the PMT dynode chain (which has a certain recovery time), in the PMT readout electronics, or a combination of both.

Both effects, of blinding and spectrum shift, have the effect of reducing the tagging efficiency of the calibration unit. The blinding creates a simple dead-time in the tagging system, a fraction of time in which the system cannot generate strobes. The spectrum shift means that low energy events in the tagging system (including some of the important 511 keV events) are shifted below the preset threshold in the tagging system, even when it is set to the minimum allowed value.

The combination of these effects produces an effective dead time in the tagging detector which can be estimated by comparison of the ground and in-flight count rates as:

$$9940 \times (1 - f_{\rm d}) = 6120$$

and hence the dead fraction $f_{\rm d} = 38\%$. The ratio of the count rates recorded in the OBCU internal spectra gives precisely the same result.

4. Calibration photon fluxes

Simulations using the GEANT4 package (Agostinelli 2003) have been used in order to estimate the event rates in the IBIS detector planes as a result of calibration source disintegrations. The calculations include the effects of (a) random coincidences between the detector plane background and OBCU tagging system and (b) the OBCU blinding estimated in the previous section.

The effect of random coincidences is to remove science events from the science data streams; the OBCU creates an effective dead-time for science data and simultaneously degrades the quality of the calibration data, which has a random sample of detector counts added to it.

Conversely, the main effect of blinding and/or loss of tagging efficiency is to divert events from the calibration datastreams into the main science data-streams (Table 1).

The predictions and observed rates in the two calibration datastreams agree reasonably well with the predicted rates. These demonstrate that the calibration lines are being divided almost equally between the science and calibration datastreams. However, the actual OBCU rate in the science data represents only a ~1% increase over background. The OBCU events leaking into the science data have a well-defined spatial and energy distribution and so may be removed during the uniformity and background correction phase of analysis (Goldwurm 2003).

5. Calibration data quality

5.1. ISGRI

The ISGRI calibration events (S2 datastream) are received at a rate of 45 c/s. The ISGRI calibration spectrum (Fig. 4) is dominated by calibration photon induced fluorescence emission from the tube and hopper, made from lead and tungsten respectively. Fluorescence is responsible for the complex of lines around PHA channel ~100. The original 511 keV flux is also detected, if only weakly, at PHA channel ~1000 and can be used for long-term recalibration of both pixel gain and energy-loss corrections.

5.2. PICsIT

PICsIT calibration events (S5 datastream) are received at a rate of 75 c/s for the detector plane as a whole and stored onboard as histograms with integration time of typically 1800 s. A typical pulse-height spectrum is shown as Fig. 5. Note that

Table 1. Predicted and measured rates from OBCU assuming 38% effective OBCU dead time (all count/s; for source activity at mission start).

Datastream	Description	511 keV	1275 keV	Continuum	Random	Total	Observed
S1	ISGRI	2.6	–	10.6	–	–	–
S2	**ISGRI calibration**	1.9	–	7.8	40.0	49.7	45
S3.0	Compton single-site	1.2	0.2	1.5	1.2	4.1	–
S3.1	Compton multi-site	0.1	0.1	0.1	0.4	0.7	–
S4.0/S7.0	PICSIT single-site science	19.6	1.8	26.8	–	–	–
S4.1/S7.1	PICSIT multi-site science	9.4	4.6	5.4	–	–	–
S5	**PICSIT calibration**	18.3	2.1	26.0	43.2	90.2	75

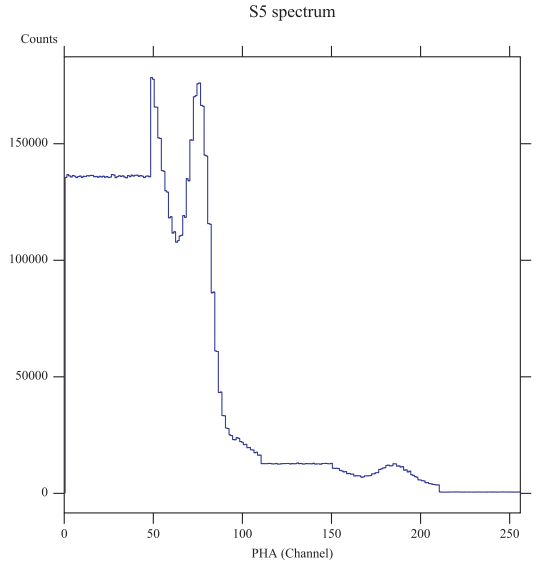

Fig. 5. Typical S5 (PICSIT calibration) spectrum, summed over all pixels and integrated for one revolution.

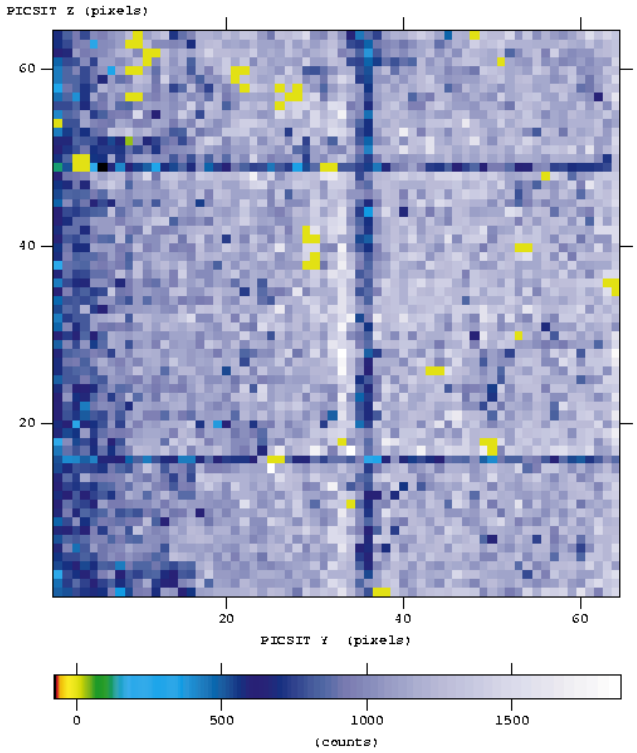

Fig. 6. Distribution of detected calibration photons across the PICsIT detector plane. The non-uniform distribution derives from a combination of source flux, detection efficiency and tagging efficiency. Note the presence of a few permanently off pixels.

the histogramming uses a variable binning to store detailed data only around the 511 keV ($PHA \sim 75$) and 1275 keV ($PHA \sim 180$) peaks.

Analysis of PICsIT calibration data may be accomplished at several levels:

- Monitoring of overall detector plane characteristics using the total spectrum for all pixels. The data quality is good enough to achieve this at ~1 hour timescales.

- Monitoring of 511 keV line position in individual pixels on timescales of 1 revolution.

- Monitoring of 1275 keV line position in individual pixels on timescales of 5 revolutions, allowing an absolute recalibration of pixels gains.

Analysis was performed on PICsIT calibration histogram data throughout the commissioning phase, and the system was seen to perform excellently, tracking the temperature (and hence gain) changes throughout each orbit in full agreement with the temperature values in housekeeping (Malaguti 2003).

6. Simulation and interpretation

The distribution of counts in coincidence with the OBCU across the PICsIT detector plane has been determined by performing background-subtraction on a PICsIT calibration data (S5) histogram. The background in the calibration histogram derives from random coincidences between the OBCU tagging system and other PICsIT events and so can be obtained by scaling of the PICsIT science data for single-site events (S7.0 datastream).

The calibration count distribution in PICsIT (Fig. 6) shows a number of features:

(a) A clear set of shadows (at $y = 36$, $z = 15$ and $z = 49$) cast by the ISGRI spider. The counting rate in these shadowed regions is reduced almost by a factor of 2.

(b) A region of enhanced counts at $y = 32$, where the edges of the PICsIT modules subtend an increased geometrical area to the OBCU.

(c) A region of reduced counts ($y < 10$). Indeed, there are hints of an overall increasing count rate towards higher y. This is contrary to expectations due to simple distance and/or solid angle effects.

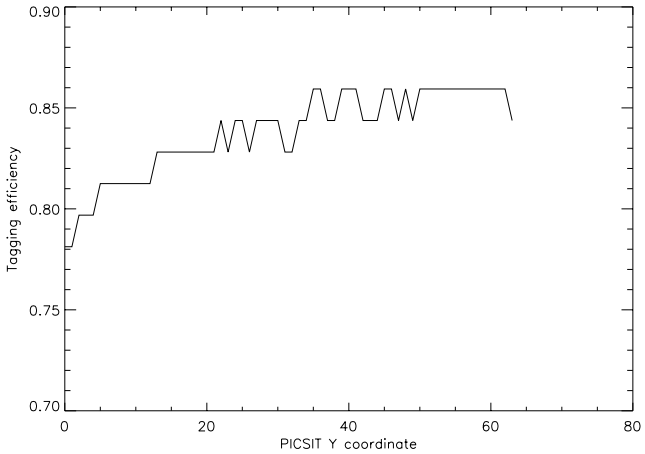

Fig. 7. Spatial variation of tagging efficiency derived from GEANT4 simulations.

This latter effect was investigated by use of more detailed monte-carlo simulations with a full implementation of the ^{22}Na decay scheme, and much better statistics revealing spatial variations in the calibration photon count distribution. These were performed using the Integral Mass Model (Ferguson 2003).

In data simulated for only OBCU events, the tagging efficiency can be derived from the fraction of events correctly passed to the S5 calibration datastream compared to the total counts. Hence:

$$\epsilon_{\rm tagging} = \frac{C_{\rm S5}}{C_{\rm S7.0} + C_{\rm S5}}, \quad (1)$$

where $C_{\rm S7.0}$ is the count rate in the PICsIT single-site science data, and $C_{\rm S5}$ is the count rate in the PICsIT calibration data.

A plot of the tagging efficiency derived in this way (Fig. 7) shows a clear systematic variation across the detector plane of ∼10%, with a sharp decline at low y coordinates. This can be understood by reference to Fig. 1; the volume of the OBCU tagging detector diametrically opposite the low-y PICsIT pixels is significantly lower than that for higher-y pixels.

7. Conclusions

The IBIS on-board calibration unit (OBCU) is generally working well, but is suffering from the effect of high-energy particle interactions which are causing both a blinding (dead-time) effect and a shift in the recorded pulse height in the active tagging system. The combined result of these two effects is a reduction of ∼38% in the tagging efficiency. This in turn leads to longer times to acquire acceptable calibration spectra, and some leakage of calibration events into the science data streams.

For ISGRI, both the direct tagged flux of 511 keV photons and secondary tagged photons (from fluoresence etc) can be used to calibrate the instrument response.

For PICsIT, the time to carry out a pixel-by-pixel recalibration at the required level of better than 1% accuracy is typically 1 orbit for the 511 keV line determination, and 5 orbits for the 1275 keV line. There are no other strong lines present in the PICsIT background, so the use of the OBCU is the only feasible method for PICsIT gain calibration.

For the veto, the line detections in the lateral modules are too weak due to absorption by intervening materials, while the OBCU lines are visible in the rear veto elements. This is the basis of the automatic veto analysis carried out at ISDC.

Acknowledgements. Thanks to the staff at LABEN Spa. for their help in the ground calibration of the IBIS calibration unit. A. J. Bird is funded by PPARC grant GR/2002/00446.

References

Agostinelli, S., Allison, J., Amako, K., et al. 2003, Nucl. Instr. Meth., A506, 250
Ferguson, C., Barlow, E. J., Bird, A. J., et al. 2003, A&A, 411, L19
Goldwurm, A., David, P., Foschini, L., et al. 2003, A&A, 411, L223
Labanti, C., Di Cocco, G., Ferro, G., et al. 2003, A&A, 411, L149
Lebrun, F., Leray, J. P., Lavocat, P., et al. 2003, A&A, 411, L141
Malaguti, G. M., Bazzano, A., Bird, A. J., et al. 2003, A&A, 411, L173
Poulsen, J. M., Sarra, P., Bird, A. J., et al. 2001, in Exploring the gamma-ray universe, ESA SP-459 (ESA publications Division), 615
Quadrini, E. M., Bazzano, A., Bird, A. J., et al. 2003, A&A, 411, L153
Segreto, A., Labanti, C., Bazzano, A., et al. 2003, A&A, 411, L215
Ubertini, P., Di Cocco, G., Lebrun, F., et al. 1996, SPIE 5-7, 2806, 246
Ubertini, P., Di Cocco, G., Lebrun, F., et al. 2003, A&A, 411, L131
Winkler, C., Courvoisier, T. J.-L., Di Cocco, G., et al. 2003, A&A, 411, L1